 doi:10.20944/preprints202012.0438.v1

Article

Linking tissue damage to hyperspectral reflectance for non-invasive monitoring of apple fruit in orchards

Alexei Solovchenko [1,2]*, Alexei Dorokhov [5], Boris Shurygin [1,3], Alexandr Nikolenko [3], Vitaly Velichko [4], Igor Smirnov [5], Dmitriy Khort [5], Aleksandr Aksenov [5], and Andrei Kuzin[1]

[1] Michurin Federal Scientific Center; andrey.kuzin1967@yandex.ru
[2] Lomonosov Moscow State University;
[3] Moscow Institute of Physics and Technology (National University); shu_b@mail.ru
[4] Stavropol Fruit Nursery Center Plodoobjedinenie "Sady Stavropolya"; vit_velichko@mail.ru
[5] Federal Scientific Agroengineering Center VIM;
* Correspondence: solovchenko@mail.bio.msu.ru; Tel.: +7-495-939-2587

Abstract: Reflected light carries ample information about biochemical composition, tissue architecture, and physiological condition of plants. Recent technical progress brought about affordable imaging hyperspectrometers (IH) providing spatially resolved spectral data on plants. The extraction of sensible information from hyperspectral reflectance images is difficult due to inherent complexity of plant tissue and canopy optics, especially when recorded by IH under ambient sunlight. We aimed at obtaining a deeper insight into plant optics as perceived by IH since there is a high demand for algorithms for fruit harvesting and grading systems equipped with computer vision and robotic systems capable of working in orchard. We report on the characteristic changes in hyperspectral reflectance accompanying the accumulation of anthocyanins in healthy fruit, pigment breakdown during sunscald and phytopathogen attacks. The measurements made outdoors with a snapshot IH were compared with traditional "point" reflectance measured with a conventional spectrophotometer under controlled illumination conditions. Most of the spectral features and patterns of plant reflectance were evident in the IH-derived reflectance images. As a step forward, a novel index for highlighting tissue damages on the background of the anthocyanin absorption, BRI-M = $(1/R_{orange} - 1/R_{red} + 1/R_{NIR})$, is suggested. Difficulties of the interpretation of fruit hyperspectral reflectance images recorded *in situ* are discussed with possible implications for plant physiology and precision horticulture practices.

Keywords: reflectance; hyperspectral imaging; pigments; damages; apple fruit

1. Introduction

Light reflected by plant carries ample information about its biochemical composition, tissue architecture, and physiological condition. Developmental changes, acclimation to environmental stresses and attacks of phytopathogens manifest themselves as specific changes in plant reflection properties [1-5]. Extraction of sensible information from reflected signal is at the core of remote and proximal sensing of vegetation but this information is difficult to extract due to inherent complexity of plant optical properties [2]. During recent decades, many approaches have been developed to obtain insights into diverse aspects of plant structure and function from multi- and hyperspectral reflectance data [2-7]. It became clear that non-destructive assessment of plant phenotypic traits requires a comprehensive understanding of plant tissue optical features and spectroscopy of pigments *in situ*. General approach implies the analysis of variation in reflectance spectra arising in response to changes in biochemical composition and plant tissue morphology to find spectral bands and/or features of maximum sensitivity to the plant trait in question such as pigment content and/or development of assorted disorders [8-12]. Still, recent studies mostly rely on the machine learning

Preprints (www.preprints.org) | NOT PEER-REVIEWED | Posted: 17 December 2020 doi:10.20944/preprints202012.0438.v1

algorithms and the observed spectral features [13,14] are not always related to the underlying biological processes such as changes in the plant tissue architecture and its biochemical composition.

Although overwhelming majority of plant tissue optics studies has been carried out on leaves [15], here we employed apple fruit featuring highly resolved reflectance spectra due localization of the bulk of pigments in a thin outer layer (so called "peel") on highly reflective tissues with a low pigment content (the "pulp") [16,17]. There is a considerable body of evidence on the use of reflectance spectroscopy for assessment of fruit condition in the literature [1,5,10,17]. Another reason of using apple as a model is its vast practical importance as a major fruit crop. In practice, it takes a lot of time and manual labor to sort out fruits with symptoms of damages and disorders having no market value and unsuitable for storage. Attempts to apply optical reflectance spectroscopy for assessment of fruit quality and their physiological state have been undertaken for decades, but the key achievements belong mostly to the field of postharvest processes e.g. grading, sorting, storing of fruit (see [1,18] and references therein). The progress in the pre-harvest non-invasive assessment is still modest although remarkable exceptions exist [5].

Current understanding of plant spectroscopy stems mostly from the "point-based" measurements with conventional spectroradiometers and spectrophotometers [18]. Recent technical progress brought about affordable imaging hyperspectrometers (IH) providing spatially resolved spectral information on plants at different scales, from plant organs (leaves and fruits) to individual plants and ecosystems [5,19]. Still, the extraction of sensible information from hyperspectral reflectance images (HRI) might be difficult due to inherent complexity of plant tissue and canopy-level optics [1]. These problems are exacerbated when the reflectance images are acquired outdoors under ambient sunlight. There were also doubts that IH can be helpful for monitoring eco-physiological responses even under controlled conditions [20]. These uncertainties and limitations stem particularly from insufficient understanding of the relationships between biochemistry and architecture features of plant tissues and their measured optical properties [21]. Solving these problems are central to confident interpretation of reflectance images, development of computer vision and robotic systems for automated fruit harvesting and grading capable of working in orchard [5,18].

Here, we report on the characteristic changes in reflectance spectra accompanying stress acclimation of and damages to apple fruit documented with an IH. Special attention was paid to the changes of the reflectance patterns and features accompanying transformation of pigments during accumulation of anthocyanins, pigment breakdown during photooxidative damage (sunscald) and cell necrosis after a phytopathogen attacks. Striving for greater confidence of interpretation of the HRI recorded *in situ*, we compared features of reflectance comprising HRI with those from reflectance spectra measured with a conventional spectrophotometer under laboratory conditions, wet biochemical analyses, and microscopic observations. Collectively, the approaches developed for the analysis of the "point-based" reflectance spectra yielded sound results also for reflectance spectra extracted from HRI recorded under ambient illumination outdoors.

2. Results

For this study, fruits bearing no visual symptoms of damage were selected (Figure S1) as well as fruit affected to a different extent by physiological disorders commonly encountered in orchards (sunburn and sunscald) and phytopathogen lesions (lesions, cell necroses, and cracks from apple scab, *Venturia inaequalis*) (Figure S2). We obtained the hyperspectral reflectance features of healthy and damaged apple fruit traceable to the characteristic features of fruit visual appearance and morphology. Towards this end, the same fruits were used for recording the HRI under ambient conditions and for conventional point-based spectral reflectance measurements.

2.1. Visual appearance and microscopic observation of healthy apple fruit tissue and damages

The studied fruits of apple, *Malus* × *domestica* Borkh displayed typical anatomy features of apple fruit (Figure 1**a**, **b**).

Preprints (www.preprints.org) | NOT PEER-REVIEWED | Posted: 17 December 2020 doi:10.20944/preprints202012.0438.v1

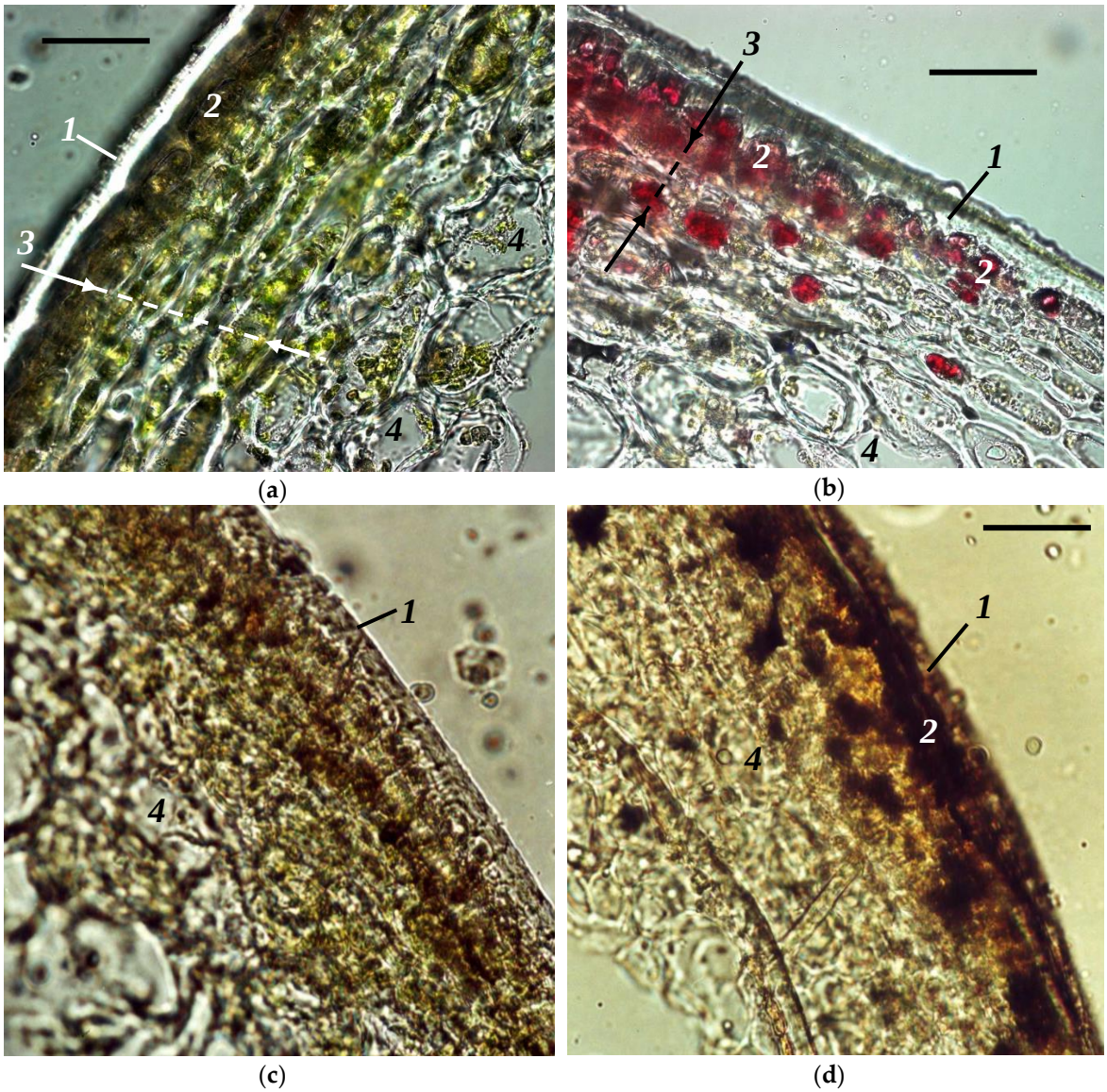

Figure 1. Anatomy and morphology of healthy (**a**-**b**) green (**a**) and red (**b**) apple fruit as well as fruit affected by (**c**) moderate sunscald and (**d**) severe cell necrosis due to scab. *1*—cuticle, *2*—epiderm, *3*—pigment-enriched compact "peel" (outer mesocarp), *4*—highly reflective "pulp" (inner mesocarp). Scale bar: 50 μm.

The fruit is covered by cuticle, the first structure of plant surface which interacts with environmental factors including solar radiation. It is a multi-layer lipophilic membrane composed by a matrix of cutin, a polymer of di- and trihydroxy fatty acids, encrusted by intracuticular waxes and covered with crystals of epicuticular waxes [22,23]. The cuticle limits transpiration, hinders phytophathogen attacks, reflects a considerable portion of incident radiation and attenuates the part of radiation entering the interior of the fruit [15], mostly due to phenolic compounds localized in the waxy layer and/or co-polymerized with cutin [16,23,24].

Below the cuticle and a single layer of epidermal cells, there were several layers of relatively small cells harboring the bulk of chloroplasts and hence fruit pigments—chlorophylls (Chl) and carotenoids (Car) as well as anthocyanins (AnC) and colorless UV-absorbing phenolics in the cell vacuoles (Figure 1). Most of the fleshy part of the apple fruit is constituted by the parenchymatous tissue composed by large cells. It has a low pigment content but incorporates numerous spaces between its cells and numerous interfaces, therefore this tissue is highly reflective [16].

Physiological diseases of various nature exemplified by sunscald [25] as well as by attacks of phytopathogens e.g. apple scab (*Venturia inaequalis*) induce breakdown of pigments apparent as gradual discoloration of the apple tissues (Fig. 2E), a considerable part of fruit crop is lost annually

Preprints (www.preprints.org) | NOT PEER-REVIEWED | Posted: 17 December 2020 doi:10.20944/preprints202012.0438.v1

as a result [26]. The extent of sunscald development is strongly dependent on cultivar, climatic conditions and agricultural practices employed [27]. The disruption of cell compartments triggers the oxidation of the vacuolar phenols by polyphenol oxidase resulting in the formation of polymeric melanin-like pigment(s) production [28] manifested by progressive browning of the fruit tissues. On the fruit tissues section, browning was evident as cell necroses and compact dark inclusions filling the protoplast of the affected cells (Figure 1**c**, **d**).

2.2. Characteristic features of healthy apple fruit reflectance

Representative visible-NIR (Vis-NIR) reflectance spectra of apple fruit taken with a conventional spectrophotometer and those extracted from the HRI are shown in Figure 2. A common feature of apple fruit is a high reflectance in the near infra-red (NIR) exerting moderate variation (75–85 % in the range 750-800 nm). A characteristic feature of the fruit bearing no visual symptoms of damages was almost flat reflectance spectrum in the NIR (720-850 nm). Notably, variation of incident flux of solar radiation is unavoidable in the measurements under ambient conditions hence the increased variation in the NIR region of the formally calculated reflectance spectra whose values occasionally exceeded unity in this range (see e.g. curves *4* in Figures 2**a**, **b**).

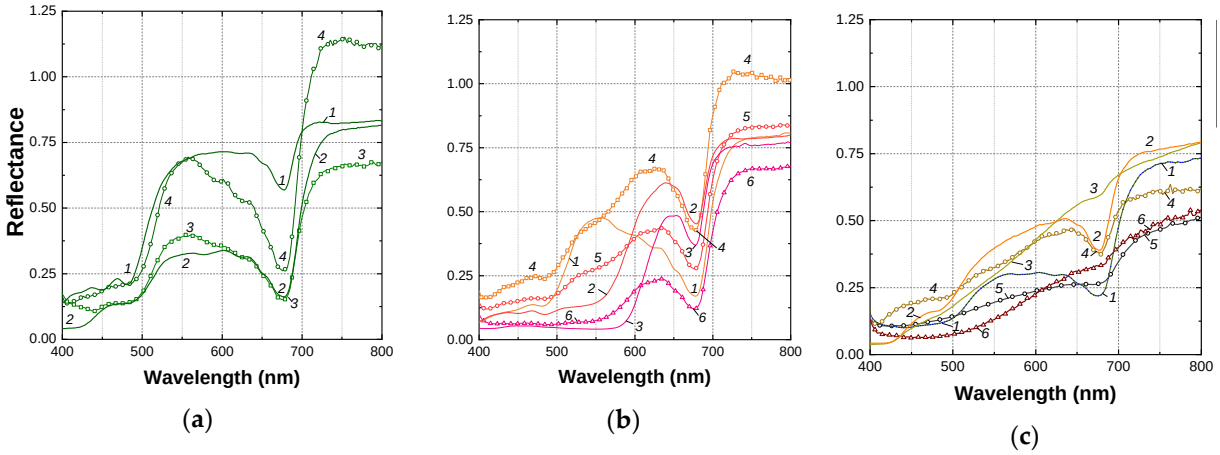

Figure 2. Reflectance spectra of (**a**) healthy green; (**b**) healthy red, and (**c**) damaged brown apple fruit surface. Spectra measured by conventional spectrophotometer are shown (line graphs, curves *1*–*3*) together with those extracted from hyperspectral reflectance images recorded at ambient illumination (symbols, curves *4*–*6*). For the details on pigment contents, see Table S1.

In the visible range, the spectral features attributable to the absorption by Chl, Car, and (in red-colored fruit) AnC were evident in the spectra of apple fruit (for detailed description of the reflectance spectral features of apples, see [16,17]). In the red part of the visible region, broad bands of Chl *a* (the pronounced minimum near 678 nm) and Chl *b* absorption (a shoulder near 650 nm) were evident in fruits regardless of their color (Figure 2**a**). In the blue-green part of the visible region of the spectrum apple fruit reflectance was low due to combined absorption of Chl, Car, and, in red-colored fruit, AnC (Figure 2**a**, **b**). Accumulation of AnC manifested itself as a characteristic shoulder near 550 nm in the case of AnC-containing red-colored fruits (Figure 2**b**). An increase in the intensity of the red coloration (and corresponding AnC content) was accompanied by a decline of reflectance in the range 675–400 nm resulting in a shift of the green edge position toward longer wavelengths and a progressive broadening of the reflectance minimum attributable to AnC. In the short-wave part of the Vis range, a decline in reflectance due to the tailing contribution of phenolic compounds possessing the main absorbance peaks in UV [16] was occasionally observed.

Notably, a fundamental feature of plant reflectance previously described for numerous plant species, the close correlation of reflectance values at 550 nm and 700 nm was evident in the spectra of yellow-green fruits lacking AnC [17,29], (r^2 = 0.95, Figure 3**b**) regardless of Chl content. In AnC-containing healthy red apple fruit reflectance at 550 nm, R_{550} was considerably lower compared to

Preprints (www.preprints.org) | NOT PEER-REVIEWED | Posted: 17 December 2020 doi:10.20944/preprints202012.0438.v1

that at 700 nm, R_{700}. As a result of AnC absorption, a strong correlation of R_{550} and R_{700} was lost in red fruit (Figure 3**b**).

2.3. Reflectance spectral signature of damaged apple fruit tissues

In this work, the reflectance spectra of the apple fruits damaged by a physiological disorder (sunscald) and a phytopathogen attack (apple scab) have been acquired using a conventional spectrophotometer (Figure 2**c,** curves *1–3*). These spectra were compared with those taken with an imaging spectrometer (Figure 2**c,** curves *4–6*). Both types of spectra possessed similar features, they also displayed a spectral signature evident of browning pigment accumulation recorded in apples affected by sunburn and superficial scald [26]. The development of damage symptoms visually apparent as discoloration and brown patches on the fruit surface brought about dramatic changes in reflectance spectra (Figures 2**c** and 3**a**). As damage progressed, reflectance of the affected fruit decreased in the whole spectral range studied (400–1000 nm) and the spectral features of Chl (in the band 620-700 nm) and Car (a sharp increase in reflectance near 500 nm) were flattened out regardless of AnC presence. A considerable decrease of reflectance occurred in the NIR, more pronounced at shorter-wavelength part of the NIR. However, the largest variation in reflectance recorded in presence of AnC occurred in the range 600–650 nm (Figure 3**a**). Overall, an increase of reflectance variation in the NIR and in the green-to-orange regions of the spectra are characteristic features of the disorders accompanied by browning [26,30]. Another important feature of reflectance changes during the development of browning was a low variation of reflectance coefficients in the band of long-wave Chl absorption maximum centered at 678 nm and in the region of strong combined absorption of all pigment in the blue-green region (400–500 nm; see Figure 3**a**).

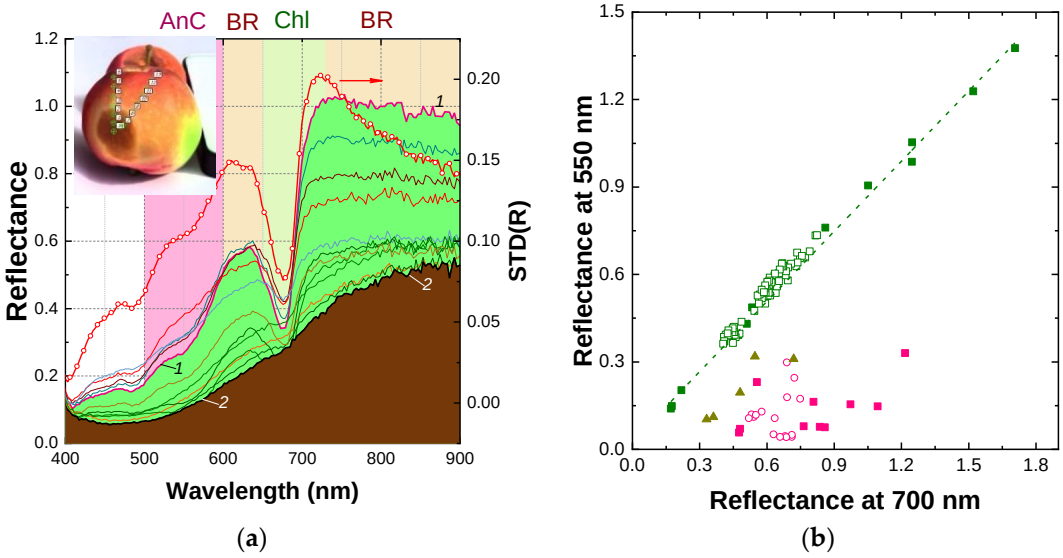

(**a**) (**b**)

Figure 3. Signature analysis of hyperspectral reflectance changes accompanying the development of browning in the apple fruit (cv. Ligol) affected by sunscald. (**a**) Representative spectra of reflectance obtained with the SPECIM IQ IH (left scale) and their standard deviation (symbols, right scale). Inset: the image of the fruit using for the measurements and the points where the spectra were extracted from the corresponding HRI; (**b**) Disturbance of the strong correlation of R_{550}^{-1} and R_{700}^{-1} typical of healthy fruit in case of red fruit (magenta symbols) and fruits affected by browning (closed triangles)

2.4. Spectral indices for the processing of hyperspectral reflectance images

To develop a sensitive optical indicator of plant damages accompanied for browning, it was necessary to select the spectral bands exhibiting (i) a high sensitivity to browning, and (ii) a minimal sensitivity to browning, but sensitive to contributions by Chl and Car. As it follows from the analysis of the reflectance spectra presented above, R_{NIR} and R_{640} exhibited a high sensitivity to browning development. Therefore, we suggested R_{640}^{-1} and R_{800}^{-1} as the terms sensitive to accumulation of

Preprints (www.preprints.org) | NOT PEER-REVIEWED | Posted: 17 December 2020 doi:10.20944/preprints202012.0438.v1

browning and R_{678}^{-1} as a term minimally sensitive to browning but sensitive to Chl content in apple [17]. Subtracting R_{678}^{-1} from the sum ($R_{640}^{-1} + R_{800}^{-1}$) allowed to construct an index that was sensitive to browning and was minimally sensitive to variation of Chl and Car contents. Reflectance at 800 nm, which exhibits low variation in healthy fruits but decreases significantly in the course of browning (Figures 2 and 3) was introduced as a term, increasing its sensitivity to browning. Finally, the modified browning reflectance index (mBRI) was suggested in the form:

$$\text{mBRI} = (R_{640}^{-1} + R_{800}^{-1}) - R_{678}^{-1}, \quad (1)$$

Healthy fruits exhibited a low mBRI (0.2-0.4) regardless of their Chl and AnC content whereas in the fruit even slightly affected by sunscald a significant increase in mBRI took place even when the fruit surface revealed no visually detectable symptoms of injury. Therefore, BRI could be used as a sensitive and efficient tool for quantitative assessment of SS and other disorders accompanying by browning as well as plant diseases affecting the close relationships between reflectances at 550 and 700 nm those are inherent in healthy apple fruit tissues. It should be noted, that the original index BRI developed for browning damage assessment [26] was not applicable for red-colored apple fruit since the presence of AnC in their peel causes a significant decrease of R_{550} interfering with the browning pigment assessment. By contrast, the suggested mBRI index performed reasonably well even in the case of AnC-containing fruit (Figures 4 and 5).

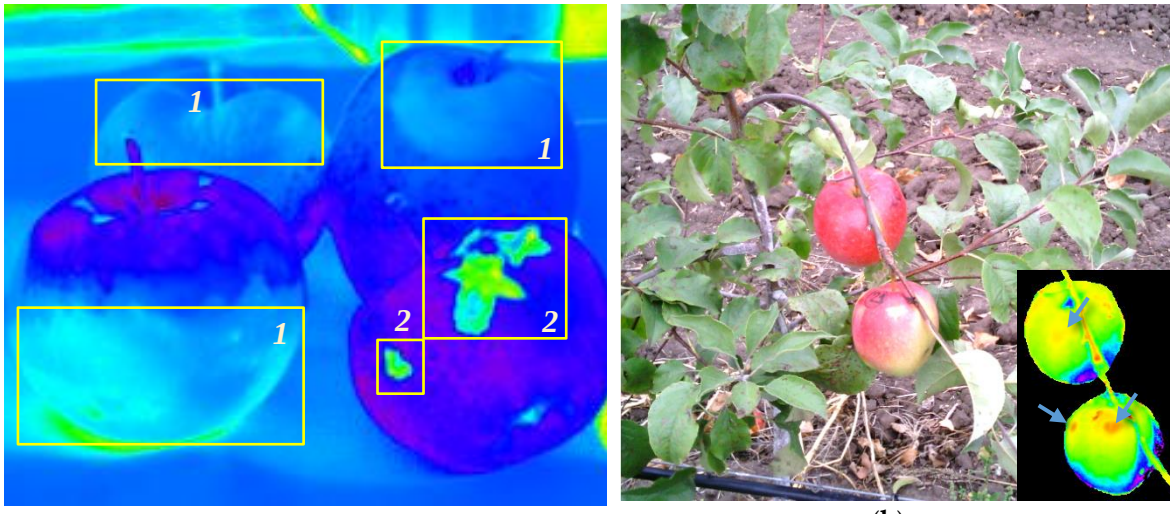

(**a**) (**b**)

Figure 4. Using the mBRI index for the detection of damages in the HRI images of Ligol apple fruit obtained at ambient illumination. (**a**) Regions of apple fruit affected by (*1*) sunscald-induced browning and (*2*) scab-induced necroses highlighted in the false-color images based on the calculated values of the mBRI index. (**b**) A RGB images reconstructed from a HRI obtained in a commercial orchard. Inset: the same scene, in masked false-color, reflecting the mBRI values revealing the onset of sunscald-induced damages (arrows)

Preprints (www.preprints.org) | NOT PEER-REVIEWED | Posted: 17 December 2020 doi:10.20944/preprints202012.0438.v1

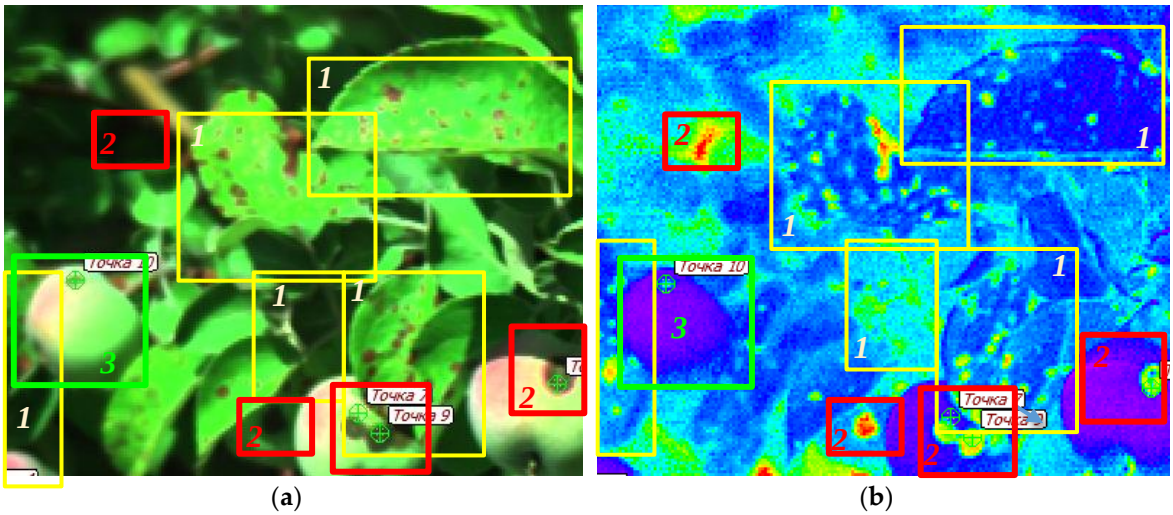

(**a**) (**b**)

Figure 5. Using the mBRI index for the detection of profound apple scab-induced damages in the HRI images of unripe Ligol apple fruit and leaves obtained at ambient illumination. (**a**) The scene in RGB composite color (as perceived by human eye and reconstructed from a HRI obtained in a commercial orchard. (**b**) The same scene in false color representing the calculated values of the mBRI index. The magenta-blue regions represent unaffected leaf and fruit area, the green-red areas are affected by the scab-induced browning. The rectangles outline the damaged leaves (*1*), fruits (*2*) as well as a healthy fruit (*3*) in **a** and **b**. Note the fruit damages (in the left) hardly visible on the RGB images due to shading but readily discernible in the mBRI index image.

3. Discussion

Reflected light signal conveys a plethora of valuable information on the integrity and physiological condition of plants including their pigment content and composition, photosynthetic activity etc. [4] Thus, the chloroplasts of mature apple peel cells harboring the Chl *a* and *b* pigments capable of photosynthesizing at a rate commensurate to that of leaves [31]. Carotenoids participate in light harvesting and being powerful antioxidants are involved in photoprotection [32]. Anthocyanins responsible for red color of apples increase their consumer acceptance [33] serving also for the protection against UV and excessive sun irradiation [34,35]. In the case of fruit, the information about the fruit carried by the reflected light also translates into the perceived fruit quality (appearance, ripeness, presence of damage) [1,18,21]. Non-destructive assessment of pigments in plant in general as well as in apple fruit is complicated by overlapping light absorption by individual pigments and non-linear relationship of reflectance vs. pigment content, especially in the bands of strong absorption [2,17]. Dramatic changes in plant tissue architecture and biochemical composition during fruit development and in response to environmental stimuli adds to this complexity [33,36]. In spite of these obstacles, efficient techniques of non-invasive assessment of fruit tissue condition have been developed [18].

Visible-Near Infrared (Vis-NIR) spectroscopy is now a widespread tool emerged from the field of remote sensing. Recent advancements in instrumentation and data analysis paved the way for the advent of affordable HRI technology. In the past two decades, it has evolved into a powerful noninvasive inspection tool; the scope of applications in postharvest quality and safety evaluation using HRI has expanded tremendously [1,18]. Still, overwhelming majority of the studies on application of Vis-NIR spectroscopy is focused on postharvest applications where the basics of the spectroscopic and chemometric theory are established and a broad range of commercially available instrumentation for packing lines is available [21]. However, the studies dedicated to the spectral imaging of fruit in the field and interpretation of reflectance images of fruit recorded under ambient conditions are much scarcer.

To bridge this gap, at least for the detection of damages associated with tissue browning, we confronted the "point-based" reflectance spectra measured with a conventional spectrophotometer with the HRI data acquired in the field. The comparative analysis has been focused on distinguishing

 doi:10.20944/preprints202012.0438.v1

the spectra of healthy fruit from those affected by physiological and phytopathogen-induced damages. Our findings presented in this paper support the compatibility of the HRI data obtained in the orchard under ambient illumination conditions using a portable IH with the fruit reflectance measured under controlled conditions with bench-top double-beam spectrophotometers. The uncertainties introduced by the variable ambient illumination were largely smoothed out by introducing reflectances in the NIR as the terms for internal normalization into the vegetation indices.

This study highlighted the effects of unfavorable weather conditions (high solar light on the background of elevated temperature) promoting the development of sunscald, a widespread photooxidative damage accompanied by characteristic changes in tissue microstructure and optical properties of the fruit [37-39]. The changes in fruit reflectance extracted from the HRI of the affected fruit regions were in line with those documented previously with "point-based" reflectance measurements and, generally, resembled the spectral changes during Chl and Car photobleaching by strong light irradiation in leaves and fruits [25,40,41]. Briefly, in sunscald-affected fruit, a simultaneous photodegradation of Car and Chl took place resulting in bleaching of the absorption bands of these pigments. At the same time, there was a decline in the reflectance in the blue-violet region of the spectrum related to the buildup of peel flavonols (mainly, rutin) in response to elevated UV fluxes coming with elevated fluxes of incident solar radiation [42,43].

Importantly, these findings enabled us to employ patterns and relationships previously documented for the point-based measurements of apple fruit reflectance to interpret the features of the HRI obtained in the field. Thus, reciprocal reflectance coefficients were successfully used for the construction of vegetation indices for leaf and fruit pigment assessment [9,17,44]. In healthy fruits, reflectance in the red or Red Edge region of the spectrum, corrected to that in the NIR, is a proxy of Chl content. In the fruits affected by browning, the spectral region sensitive to browning pigments was shifted to the yellow-orange region where absorption of AnC and Chl is low but the absorption of the browning pigments is significant. Since Chl contribute to R_{550} and even more to $R_{600–650}$, this contribution can be compensated for using reciprocal reflectance in the red, e.g R_{678} as it was done in the mBRI index suggested in this study (Equation 1). The resulting index allowed to distinguish the regions of fruit surface affected by sunscald and scab-induced necroses in HRI (Figures 4 and 5). Previously we analyzed characteristic changes in fruit tissue reflectance accompanying the development of diverse damages manifesting itself as tissue browning [26]. It was concluded at that time that browning symptoms are hard to detect via reflectance in case of red-colored fruit containing AnC pigments due to a considerable overlap of the absorption of the brown pigments and those of AnC. In this work we found an approach to monitor damage-induced browning in red AnC-containing fruit (Figures 4, 5). Employment of this index for a more quantitative assessment of the degree of lesion will require its calibration vs. accepted in practice damage scores. Overall, the HRI recorded with a shapshot IH under ambient illumination conditions captured the typical spectral features discriminating healthy fruit from those affected by the physiological and fungal diseases in sufficient detail.

4. Materials and Methods

4.1. Plant material

Fruit of apple (*Malus* × *domestica* Borkh.) (n = 50) cultivars "Golden Delicious" (green-colored), "Ligol" and "Gala" (red-colored) were with or without symptoms of damage by sunscald or apple scab were visually selected used. Fruit were grown either at an experimental orchard of Michurin Federal Scientific Center (Michurinsk, Tambov region, Russia) or in the production orchard of the "Sady Karachaevo-Cherkesii" fruit growing company (Karachay-Cherkess Republic, Russia). Depending on the measurement type, the fruit were imaged while they attached to the tree or within one hour after picking. For microscopic investigation and biochemical assays, the fruits were transferred to the lab and studied within two hours from picking.

4.2. Pigment assay

Preprints (www.preprints.org) | NOT PEER-REVIEWED | Posted: 17 December 2020 doi:10.20944/preprints202012.0438.v1

The assay of total Chl, Car, AnC, and Flv in an extract from apple sample zone used for reflectance measurements was carried out essentially as described in [45]. Briefly, fruit peel disks (total area of 3.8 cm^2, thickness ca. 1 mm) were ground in chloroform–methanol (2:1, vol/vol) in the presence of 100 mg MgO. After completion of extraction, homogenates were filtered through a pre-soaked with the chloroform–methanol mixture paper filter, and distilled water (1/5 of total extract volume) was added. Then extracts were centrifuged at 3000 *g* for 10 min until phase separation. Total Chl and Car concentrations were quantified spectrophotometrically in lower (chloroform) phase using coefficients reported by Wellburn [46]. The upper (water–methanol) phase was used for assay of total Flv, which were quantified spectrophotometrically using the band around 358 nm where Flv exert the dominant contribution to the absorption and molar absorption coefficient ε_{358} = 25.4 mM^{-1} cm^{-1} determined for rutin in 80% aqueous methanol. After determination of Flv the water–methanol phase was acidified with HCl (final concentration of HCl = 0.1 %) and used for quantification of anthocyanins by measuring absorbance at 530 nm absorption coefficient of 30 mM^{-1} cm^{-1} [47] was accepted. Pigment content were expressed per unit fruit surface area.

4.3. Light microscopy

The light microphotographs of hand-made cross-sections of fruit peel samples were taken with an Axioscope (Carl Zeiss, Jena, Germany) microscope fitted with a MRC digital camera (Carl Zeiss, Germany).

4.4. Spectral reflectance measurements

4.4.1. Reflectance spectra measurement with a conventional spectrophotometer

Diffuse reflectance spectra of apple fruit were recorded at 400-800 nm range with a Agilent Cary Bio 300 (Agilent, USA) spectrophotometer equipped with an integrating sphere attachment (internal diameter 100 mm) against spectralon plate as a 100% reflectivity standard.

4.4 Hyperspectral reflectance imaging

The hyperspectral reflectance data-containing images were captured with a snapshot imaging hyperspectrometer IQ (SPECIM, Finland). For each pixel of the hyperspectral image (512 × 512 pixels), a reflectance spectrum (spectral range 400–1000 nm; spectral resolution 1 nm) was recorded against a reflectivity standard made of Spectralon under ambient illumination.

5. Conclusions and outlook

Here, we confronted the patterns of spectral reflectance recorded with the established "point-based" spectrophotometry under controlled illumination conditions with those acquired with a novel imaging hyperspectrometer-based approach under ambient conditions in the field. Both approaches provided sufficient detail on reflectance patterns characteristic of AnC accumulation, photooxidative injury (sunscald), and cell necrosis after phytopathogen attacks. Particularly, the fundamental correlation of reflectances at 550 nm and 700 nm (and loss thereof in the red and/or damaged fruit) was discovered in the reflectance spectra extracted from HRI. Despite the difficulties of reflected signal normalization under outdoor conditions, the spectral data originating from the HRI captured in the field can be processed within the framework earlier developed for the analysis of the "point-based" apple fruit spectra and, more generally, vegetation reflectance spectra [29,42]. The validity of this approach is supported by the possibility to construct a modified browning reflectance index, BRI-M. This index was suggested in form of BRI-M = $(1/R_{Orange} - 1/R_{Red} + 1/R_{NIR})$ provided for a detection of damages manifesting themselves as tissue browning on the hyperspectral images even in AnC-containing red fruit. Our findings facilitate the extending the HRI-based proximal monitoring beyond the postharvest technology domain further to industrial apple orchards complementing the modern machine learning-based approaches. Still, more research is required to make it happen. On-tree

ripeness assessment taking into account the inherent heterogeneity of fruit physiological condition constitutes examples of hot problems that can be potentially solved using the HRI methodology.

Supplementary Materials: The following are available online at www.mdpi.com/xxx/s1, Figure S1: Typical RGB photos of the studied (a) red-colored "Gala" and (b) green-colored "Golden Delicious" healthy fruits on the trees made with a viewfinder camera of the SPECIM IQ snapshot imaging hyperspectrometer, Figure S1: A typical RGB image calculated from the HRI of the fruits with the regions unaffected and affected by the damages taken under outdoors illumination conditions, Table S1: Average pigment content of the apple fruits studied in this work.

Author Contributions: Conceptualization, A.S. and B.S.; methodology, A.S.; software, B.S.; validation, I.S., A.A. and D.Kh.; formal analysis, I.S.; investigation, A.N.; resources, V.V. and A.D.; data curation, A.A.; writing—original draft preparation, A.S.; writing—review and editing, all authors; visualization, A.N. All authors have read and agreed to the published version of the manuscript.

Funding: This research was supported by a grant of the Ministry of Science and Higher Education of the Russian Federation for large scientific projects in priority areas of scientific and technological development (grant number 075-15-2020-774).

Acknowledgments: invaluable support of Mr. Aidyn Shirinov (head of LLC "Sady Stavropolya", Russia) and Dr. Mikhail Akimov (head of Michurin Federal Scientific Centre, Russia) is gratefully acknowledged.

Conflicts of Interest: The authors declare no conflict of interest. The funders had no role in the design of the study; in the collection, analyses, or interpretation of data; in the writing of the manuscript, or in the decision to publish the results.

References

1. Lu, R.; Van Beers, R.; Saeys, W.; Li, C.; Cen, H. Measurement of optical properties of fruits and vegetables: A review. *Postharvest Biology and Technology* **2020**, *159*, doi:10.1016/j.postharvbio.2019.111003.
2. Gitelson, A.; Solovchenko, A.; Viña, A. Foliar absorption coefficient derived from reflectance spectra: A gauge of the efficiency of in situ light-capture by different pigment groups. *Journal of Plant Physiology* **2020**, *254*, 153277.
3. Fu, P.; Meacham-Hensold, K.; Guan, K.; Wu, J.; Bernacchi, C. Estimating photosynthetic traits from reflectance spectra: A synthesis of spectral indices, numerical inversion, and partial least square regression. *Plant Cell Environ* **2020**, 10.1111/pce.13718, doi:10.1111/pce.13718.
4. Solovchenko, A.; Yahia, E.M.; Chen, C. Pigments. In *Postharvest Physiology and Biochemistry of Fruits and Vegetables*, Elsevier: 2019; pp. 225-252.
5. Sabzi, S.; Abbaspour-Gilandeh, Y.; García-Mateos, G.; Ruiz-Canales, A.; Molina-Martínez, J.; Arribas, J. An Automatic Non-Destructive Method for the Classification of the Ripeness Stage of Red Delicious Apples in Orchards Using Aerial Video. *Agronomy* **2019**, *9*, doi:10.3390/agronomy9020084.
6. Cendrero-Mateo, M.; Muller, O.; H, A.; Burkart, A.; Gatzke, S.; Janssen, B.; Keller, B.; Körber, N.; Kraska, T.; Matsubara, S., et al. Field Phenotyping: Concepts and Examples to Quantify Dynamic Plant Traits across Scales in the Field. In *Terrestrial ecosystem research infrastructures: Challenges and opportunities*, Chabbi, A., Loescher, H., Eds. CRC Press: Boca Raton, 2017; 10.1201/9781315368252-4pp. 53-82.
7. Féret, J.B.; Gitelson, A.A.; Noble, S.D.; Jacquemoud, S. PROSPECT-D: Towards modeling leaf optical properties through a complete lifecycle. *Remote Sensing of Environment* **2017**, *193*, 204-215, doi:10.1016/j.rse.2017.03.004.
8. Kira, O.; Nguy-Robertson, A.L.; Arkebauer, T.J.; Linker, R.; Gitelson, A.A. Informative spectral bands for remote green LAI estimation in C3 and C4 crops. *Agricultural and Forest Meteorology* **2016**, *218*, 243-249.

9. Gitelson, A.; Viña, A.; Solovchenko, A.; Arkebauer, T.; Inoue, Y. Derivation of canopy light absorption coefficient from reflectance spectra. *Remote Sensing of Environment* **2019**, *231*, 111276.
10. Grandón, S.; Sanchez-Contreras, J.; Torres, C.A. Prediction models for sunscald on apples (Malus domestica Borkh.) cv. Granny Smith using Vis-NIR reflectance. *Postharvest Biology and Technology* **2019**, *151*, 36-44, doi:10.1016/j.postharvbio.2019.01.012.
11. Saeys, W.; Nguyen Do Trong, N.; Van Beers, R.; Nicolaï, B.M. Multivariate calibration of spectroscopic sensors for postharvest quality evaluation: A review. *Postharvest Biology and Technology* **2019**, *158*, doi:10.1016/j.postharvbio.2019.110981.
12. Poblete, T.; Camino, C.; Beck, P.S.A.; Hornero, A.; Kattenborn, T.; Saponari, M.; Boscia, D.; Navas-Cortes, J.A.; Zarco-Tejada, P.J. Detection of Xylella fastidiosa infection symptoms with airborne multispectral and thermal imagery: Assessing bandset reduction performance from hyperspectral analysis. *ISPRS Journal of Photogrammetry and Remote Sensing* **2020**, *162*, 27-40, doi:10.1016/j.isprsjprs.2020.02.010.
13. Tripathi, M.K.; Maktedar, D.D. A role of computer vision in fruits and vegetables among various horticulture products of agriculture fields: A survey. *Information Processing in Agriculture* **2019**, 10.1016/j.inpa.2019.07.003, doi:10.1016/j.inpa.2019.07.003.
14. Sadeghi-Tehran, P.; Virlet, N.; Ampe, E.M.; Reyns, P.; Hawkesford, M.J. DeepCount: In-Field Automatic Quantification of Wheat Spikes Using Simple Linear Iterative Clustering and Deep Convolutional Neural Networks. *Front Plant Sci* **2019**, *10*, 1176, doi:10.3389/fpls.2019.01176.
15. Vogelmann, T. Plant tissue optics. *Annual Review of Plant Biology* **1993**, *44*, 231-251.
16. Solovchenko, A.; Merzlyak, M. Optical properties and contribution of cuticle to UV protection in plants: experiments with apple fruit. *Photochem Photobiol Sci* **2003**, *2*, 861-866.
17. Merzlyak, M.; Solovchenko, A.; Gitelson, A. Reflectance spectral features and non-destructive estimation of chlorophyll, carotenoid and anthocyanin content in apple fruit. *Postharvest Biology and Technology* **2003**, *27*, 197-212.
18. Walsh, K.B.; Blasco, J.; Zude-Sasse, M.; Sun, X. Visible-NIR 'point' spectroscopy in postharvest fruit and vegetable assessment: The science behind three decades of commercial use. *Postharvest Biology and Technology* **2020**, *168*, doi:10.1016/j.postharvbio.2020.111246.
19. Astor, T.; Dayananda, S.; Nautiyal, S.; Wachendorf, M. Vegetable Crop Biomass Estimation Using Hyperspectral and RGB 3D UAV Data. *Agronomy* **2020**, *10*, doi:10.3390/agronomy10101600.
20. Pieters, O.; De Swaef, T.; Lootens, P.; Stock, M.; Roldán-Ruiz, I.; wyffels, F. Limitations of snapshot hyperspectral cameras to monitor plant response dynamics in stress-free conditions. *Computers and Electronics in Agriculture* **2020**, *179*, doi:10.1016/j.compag.2020.105825.
21. Lu, Y.; Saeys, W.; Kim, M.; Peng, Y.; Lu, R. Hyperspectral imaging technology for quality and safety evaluation of horticultural products: A review and celebration of the past 20-year progress. *Postharvest Biology and Technology* **2020**, *170*, doi:10.1016/j.postharvbio.2020.111318.
22. Holloway, P.; Cutler, D.; Alvin, K.; Price, C. Structure and histochemistry of plant cuticular membranes: an overview. In *The plant cuticle*, Cutler, D., Alvin, K., Price, C., Eds. Academic Press: London, 1982; pp. 1-32.
23. Liakopoulos, G.; Stavrianakou, S.; Karabourniotis, G. Analysis of epicuticular phenolics of Prunus persica and Olea europaea leaves: evidence for the chemical origin of the UV-induced blue fluorescence of stomata. *Annals of botany* **2001**, *87*, 641-648.

24. Karabourniotis, G.; Bornman, J. Penetration of UV-A, UV-B and blue light through the leaf trichome layers of two xeromorphic plants, olive and oak, measured by optical fibre microprobes. *Plant Physiology* **1999**, *105*, 655-661.
25. Merzlyak, M.; Solovchenko, A.; Chivkunova, O. Patterns of pigment changes in apple fruits during adaptation to high sunlight and sunscald development. *Plant Physiology et Biochemistry* **2002**, *40*, 679-684.
26. Chivkunova, O.B.; Solovchenko, A.; Sokolova, S.; Merzlyak, M.N.; Reshetnikova, I.; Gitelson, A.A. Reflectance Spectral Features and Detection of Superficial Scald–induced Browning in Storing Apple Fruit. *Journal of Russian Phytopathological Society* **2001**, *2*, 73-77.
27. Ferguson, I.; Volz, R.; Woolf, A. Preharvest factors affecting physiological disorders of fruit. *Postharvest Biology and Technology* **1999**, *15*, 255-262.
28. Vaughn, K.; Duke, S. Function of polyphenol oxidase in higher plants. *Physiologia Plantarum* **1984**, *60*, 106-112.
29. Gitelson, A.; Solovchenko, A. Generic algorithms for estimating foliar pigment content. *Geophysical Research Letters* **2017**, *44*, 9293-9298.
30. McClure, W. A spectrophotometric technique for studying the browning reaction in tobacco. *Trans. ASAE* **1975**, *18*, 380-383.
31. Blanke, M.; Lenz, F. Fruit photosynthesis. *Plant, Cell & Environment* **1989**, *12*, 31-46.
32. Takaichi, S. Tetraterpenes: Carotenoids. In *Natural Products*, Ramawat, K.G., Mérillon, J.-M., Eds. Springer Berlin Heidelberg: 2013; 10.1007/978-3-642-22144-6_141pp. 3251-3283.
33. Saure, M. External control of anthocyanin formation in apple: a review. *Scientia Horticulturae* **1990**, *42*, 181-218.
34. Solovchenko, A.; Merzlyak, M. Screening of visible and UV radiation as a photoprotective mechanism in plants. *Russian Journal of Plant Physiology* **2008**, *55*, 719-737.
35. Liakopoulos, G.; Nikolopoulos, D.; Klouvatou, A.; Vekkos, K.-A.; Manetas, Y.; Karabourniotis, G. The photoprotective role of epidermal anthocyanins and surface pubescence in young leaves of grapevine (Vitis vinifera). *Annals of botany* **2006**, *98*, 257-265.
36. Gross, J. *Pigments in fruits*; Orlando, Flo., Academic Press: 1987.
37. Andrews, P.; Fahy, D.; Foyer, C. Relationships between fruit exocarp antioxidants in the tomato (Lycopersicon esculentum) high pigment-1 mutant during development. *Physiologia Plantarum* **2004**, *120*, 519-528.
38. Andrews, P.; Johnson, J. Physiology of sunburn development in apples. *Good Fruit Grower* **1996**, *47*, 33-36.
39. Andrews, P.; Johnson, J.; Fahy, D. Protection against sunscald in apple fruits by the ascorbate-glutathione cycle. In Proceedings of International congress on science and horticultural interfaces and interactions (IHC); pp. 2-7.
40. Merzlyak, M.; Gitelson, A.; Pogosyan, S.; Lekhimena, L.; Chivkunova, O. Light-induced pigment degradation in leaves and ripening fruits studied in situ with reflectance spectroscopy. *Physiologia Plantarum* **1998**, *104*, 661-667.
41. Merzlyak, M.N.; Solovchenko, A.E. Photostability of pigments in ripening apple fruit: a possible photoprotective role of carotenoids during plant senescence. *Plant Science* **2002**, *163*, 881-888, doi:10.1016/s0168-9452(02)00241-8.
42. Solovchenko, A.; Schmitz-Eiberger, M. Significance of skin flavonoids for UV-B-protection in apple fruits. *J Exp Bot* **2003**, *54*, 1977-1984, doi:10.1093/jxb/erg199

erg199 [pii].

43. Merzlyak, M.N.; Solovchenko, A.E.; Smagin, A.I.; Gitelson, A.A. Apple flavonols during fruit adaptation to solar radiation: spectral features and technique for non-destructive assessment. *J Plant Physiol* **2005**, *162*, 151-160.
44. Gitelson, A.; Solovchenko, A. Non-invasive quantification of foliar pigments: Possibilities and limitations of reflectance-and absorbance-based approaches. *Journal of Photochemistry and Photobiology B: Biology* **2018**, *178*, 537-544.
45. Gitelson, A.; Chivkunova, O.; Zhigalova, T.; Solovchenko, A. In situ optical properties of foliar flavonoids: Implication for non-destructive estimation of flavonoid content. *Journal of plant physiology* **2017**, *218*, 258-264.
46. Wellburn, A. The spectral determination of chlorophyll a and chlorophyll b, as well as total carotenoids, using various solvents with spectrophotometers of different resolution. *Journal of Plant Physiology* **1994**, *144*, 307-313.
47. Strack, D.; Wray, V. Anthocyanins. In *Methods in plant biochemistry*, Harborne, J., Dey, P., Eds. Acad. Press: 1989; Vol. 1, pp. 325–356.

Preprints (www.preprints.org) | NOT PEER-REVIEWED | Posted: 17 December 2020 doi:10.20944/preprints202012.0438.v1

Supplementary figures

(**a**) (**b**)

Figure S1. Typical RGB photos of the studied (**a**) red-colored "Gala" and (**b**) green-colored "Golden Delicious" healthy fruits on the trees made with a viewfinder camera of the SPECIM IQ snapshot imaging hyperspectrometer (see Methods). Note the 100% reflectivity standard above the trees.

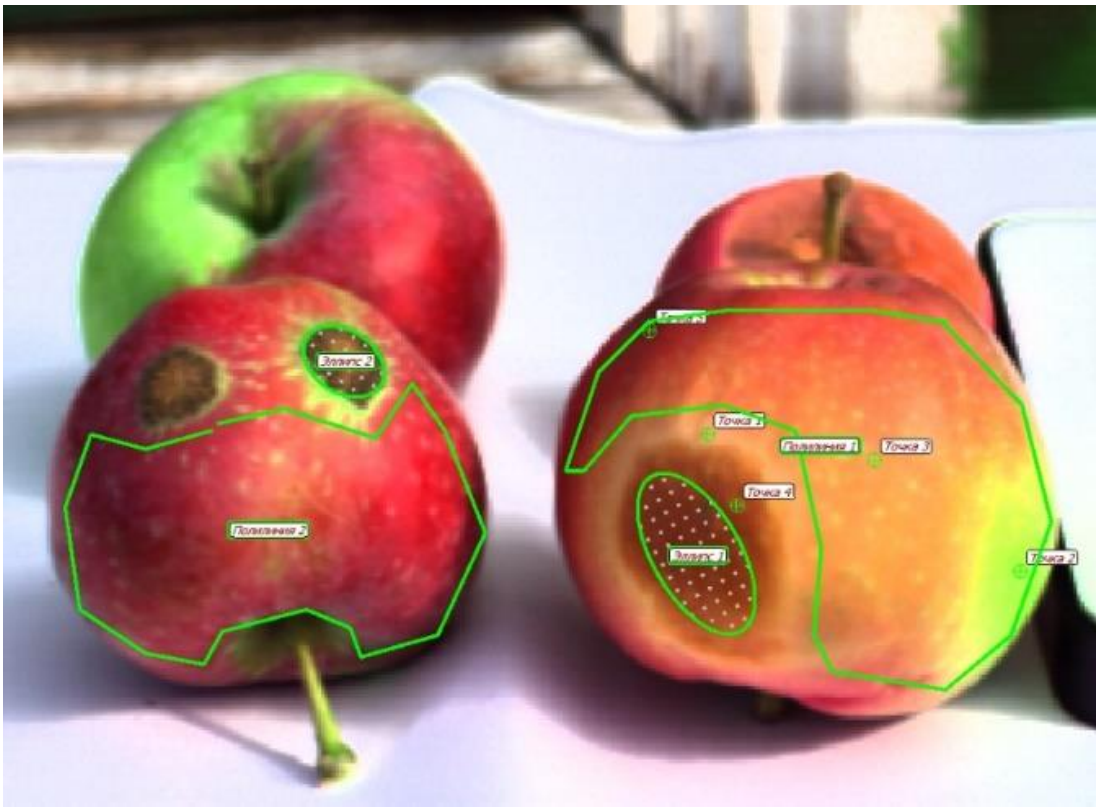

Figure S2. A typical RGB image calculated from the HRI of the fruits with the regions unaffected and affected by the damages taken under outdoors illumination conditions. The regions are marked for the sampling of spectral data (for explanation, see text).

Table S1. Average pigment content of the apple fruit studied in this work.

Preprints (www.preprints.org) | NOT PEER-REVIEWED | Posted: 17 December 2020 doi:10.20944/preprints202012.0438.v1

Pigment group	Fruit condition				
	Healthy green	Healthy red	Sunscald (mild)	Sunscald (severe)	Scab-affected
Chlorophylls	11.4±0.5[1]	10.6±0.8	6.7±1.2	1.5±0.8	0.5±0.3
Carotenoids	2.9±0.3	3.4±0.5	5.9±1.8	3.8±2.1	1.2±0.8
Anthocyanins	0.3±0.1	46±8.7	12±3.9	5.3±0.4	2.7±1.3
Flavonols	39.1±5.2	169±13.4	235±38.0	25.6±4.8	15±3.5

[1] Averages ± STD (n = 15) are shown.